

COMBINED FIXED-ORDER AND EFFECTIVE-THEORY APPROACH
TO $b\bar{b}$ SUM RULES**Adrian Signer***Institute for Particle Physics Phenomenology
Durham, DH1 3LE, England***Abstract**

We combine the fixed-order evaluation of the $b\bar{b}$ sum rules with a non-relativistic effective-theory approach. The combined result for the n -th moment includes all terms suppressed with respect to the leading-order result by $\mathcal{O}(\alpha_s^3)$ and $\mathcal{O}((\alpha_s\sqrt{n})^l\alpha_s^2)$, counting $\alpha_s\sqrt{n} \sim 1$. When compared to experimental data, the moments thus obtained show a remarkable consistency and allow for an analysis in the whole range $1 \leq n \lesssim 16$.

1 Introduction and outline

Near threshold, the cross section for the production of a $b\bar{b}$ pair, $\sigma(e^+e^- \rightarrow b\bar{b})$, is extremely sensitive to the mass of the bottom quark m_b , which allows for a precise determination of m_b . This is usually done by considering sum rules [1] and defining the n -th moment

$$M_n \equiv \int_0^\infty \frac{ds}{s^{n+1}} R_{b\bar{b}}(s) = \frac{12\pi^2 e_b^2}{n!} \left(\frac{d}{dq^2} \right)^n \Pi(q^2)|_{q^2=0} \quad (1)$$

where $\Pi(q^2)$ is the vacuum polarization, $e_b = -1/3$ the electric charge of the bottom quark and $R_{b\bar{b}}(s) \equiv \sigma(e^+e^- \rightarrow b\bar{b})/\sigma(e^+e^- \rightarrow \mu^+\mu^-)$ the normalized cross section. In order to extract m_b , the theoretical evaluation of M_n is compared to the experimental value. From the experimental point of view, the moment obtains contributions from the six Υ bound states and from the continuum cross section above threshold. For increasing n , the contribution from the experimentally poorly known continuum cross section becomes less and less relevant due to the suppression $1/s^{n+1}$. As for the choice of the parameter n , there are two complementary approaches. Either n is assumed to be rather small, i.e. $n \lesssim 4$ in which case $\Pi(q^2)$ is computed in a standard weak coupling fixed-order approach or n is assumed to be rather large $n \gtrsim 8$ in which case the moments are evaluated in a non-relativistic effective-theory approach.

In the standard fixed-order (FO) approach, the vacuum polarization is written as

$$\Pi(q^2) = \frac{N_c}{(4\pi)^2} \sum_{n \geq 0} C_n \left(\frac{q^2}{4m_b^2} \right)^n \quad (2)$$

where $N_c = 3$ is the colour factor and the coefficients C_n are evaluated as a series in the strong coupling α_s . These coefficients depend on the mass scheme that is used. We will indicate this dependence by a label X , i.e. m_X denotes the bottom quark mass in a particular scheme and $C_{n,X}$ are the corresponding coefficients. From the knowledge of $C_{n,X}$, the moments are obtained as

$$M_{n,X} = \frac{3}{4} N_c e_b^2 \frac{1}{(2m_X)^{2n}} C_{n,X} \quad (3)$$

Being observables, the moments should be scheme independent. However, since the perturbative series is truncated, there is a residual scheme dependence left in M_n which again is indicated by the label X . The coefficients C_n have been computed up to $\mathcal{O}(\alpha_s^2)$, i.e. three loops for $n \leq 8$ in Ref. [2] and up to $n \leq 30$ in Ref. [3]. The four-loop coefficient is known for $n = 0, 1$ [4, 5] and these results have been used to obtain precise values for $\overline{m} \equiv m_{\overline{\text{MS}}}$, the bottom quark mass in the $\overline{\text{MS}}$ -scheme [5, 6].

At $l + 1$ loops, the coefficients C_n contain terms $n^{-3/2}(\alpha_s\sqrt{n})^l$. Thus, if n increases, the higher-order terms become more important and for $\sqrt{n} \sim \alpha_s^{-1}$ the standard fixed-order approach completely fails. This is related to the fact that in a strict expansion in α_s the theory does not contain bound states. Given that for increasing n the moments are dominated by the lowest resonances it is thus not surprising that a FO approach does not very well describe M_n for large n . As a consequence, mass determinations using this approach [7, 8, 5, 6] use small values of n .

In order to describe the weak coupling bound states in the $b\bar{b}$ system, we have to consider the non-relativistic sum rule. The starting point is the solution to the Schrödinger equation describing a non-relativistic $b\bar{b}$ pair interacting through the Coulomb potential $-C_F\alpha_s/r$ with $C_F = 4/3$ a colour factor. This resums all terms of the form $v(\alpha_s/v)^l$ in $R_{b\bar{b}}$, where v is the small velocity of the heavy quarks and, therefore, resums all terms of the form $n^{-3/2}(\alpha_s\sqrt{n})^l$ in M_n . Higher order corrections in α_s as well as v are taken into account using Quantum Mechanics perturbation theory and counting $\alpha_s \sim v$. This is done most efficiently in the framework of an effective theory (for a review see Ref. [9]). Within the effective-theory (ET) approach the next-to-next-to-leading order (NNLO) corrections to the non-relativistic sum rules, including all terms suppressed by $\alpha_s^2 \sim \alpha_s/\sqrt{n} \sim n^{-1}$ with respect to the leading-order result, have been computed and used to determine the bottom quark mass [10]. The theoretical predictions can be improved upon by resummation of large logarithms [11] of the form $(\alpha_s \log v)^l$ and including these terms in the non-relativistic sum rule leads to a much more robust determination of the bottom quark mass [12].

Ultimately the most interesting quantity is \overline{m} , the bottom quark mass in the $\overline{\text{MS}}$ -scheme. Using non-relativistic sum rules, \overline{m} has to be determined in two steps. First, a so called threshold mass [13, 14, 15] has to be used which is closely related to the pole mass but accounts for the cancellation of the renormalon ambiguity in the observable M_n . In a second step, the threshold mass is related to \overline{m} . Using this approach, the moments can be determined reliably for large values of n , as long as non-perturbative contributions are not too important. However, for small values of n this approach breaks down due to the neglect of terms suppressed for large n or small v . As an example consider terms of order $\alpha_s^0 v^3$ in $R_{b\bar{b}}$ which are kept at NNLO in an ET approach, whereas terms of order $\alpha_s^0 v^5$ are dropped. These terms result in contributions of the order $\alpha^0 n^{-5/2}$ and $\alpha^0 n^{-7/2}$ respectively in M_n . It is clear that the latter are suppressed in the non-relativistic sum rule, i.e. for large n , but their neglect invalidates the $n \rightarrow 1$ limit of the result obtained in the non-relativistic approach.

Large n and small n applications of the sum rules and the corresponding determinations of m_b both have their advantages and disadvantages. From the large n point of view, one advantage is that due to $M_n \sim 1/(2m_b)^{2n}$ the moments

are much more sensitive to the bottom quark mass for large n . Also, they are virtually insensitive to the continuum contribution. Since this contribution is experimentally only known very poorly, small n determinations of the bottom quark mass crucially rely on the precise treatment of the data in the threshold region and have to use perturbative QCD input for $R_{b\bar{b}}$ above threshold. Given that the experimental error in the m_b determination for small n is dominant, rather subtle changes in the treatment can have significant effects on the extracted value of m_b and, in particular, its error. On the other hand, the perturbative series is much better behaved for small n . In fact, the non-relativistic sum rules suffers from very large corrections and even though the resummation of the logarithms substantially improves the behaviour of the perturbative series, the situation is far from ideal, and the dominant error still comes from the neglect of higher-order corrections. For completeness we mention again that in the large n approach \overline{m} cannot be obtained directly but only through the intermediate use of a threshold mass. However, this is not necessarily a disadvantage, since threshold masses are important and useful in their own right.

It is natural to ask whether it is not preferable to combine both approaches and perform an all n analysis of the sum rule. Since the two approaches use different techniques and are sensitive to rather different experimental input it certainly would give increased credibility if the extracted value of m_b varies very little with n , and it would allow to get a better handle on the determination of its error. The choice of n in such a combined analysis is only limited by the non-perturbative corrections. In order to get an estimate of the importance of these corrections it is useful to consider the contribution of the gluon condensate to the sum rule [16, 17]. Even though this contribution grows rapidly with n , for realistic values of the gluon condensate it is below 0.1% for $n \leq 12$ and reaches about 1% for $n = 16$. It is thus legitimate to neglect non-perturbative corrections to the b -quark sum rules as long as n is not chosen to be too large.

In this paper we consider the first 16 moments, starting in Section 2 with the fixed-order approach. Even though the large- n behaviour of the FO results is better than anticipated, will find the expected problems for large n and turn in Section 3 to the non-relativistic sum rule in order to illustrate its behaviour as a function of n . Finally, in Section 4, we combine the two approaches by adding to the non-relativistic sum rules all terms order α_s^3 that have been missed. As we will see this allows to obtain a consistent description of M_n for $1 \leq n \leq 16$. We refrain from presenting another extraction of m_b , since all theory input used in this analysis has already been used for a bottom mass determination [5, 6, 12]. The main aim of the paper is to establish the fact that a future analysis, once further improved theoretical results and hopefully better experimental data is available, should consider the full range of n in order to get a better control of the different systematic uncertainties.

2 Fixed order results, small n

In a fixed-order approach, $M_{n,X}$ can be written as in Eq. (3) and the coefficient $C_{n,X}$ has the structure

$$\begin{aligned} C_{n,X} &= C_{n,X}^{(0)} + \frac{\alpha_s}{\pi} C_{n,X}^{(1)} + \frac{\alpha_s^2}{\pi^2} C_{n,X}^{(2)} + \frac{\alpha_s^3}{\pi^3} C_{n,X}^{(3)} + \dots \\ &= C_{n,X}^{(0)} + \frac{\alpha_s}{\pi} \left(C_{n,X}^{(10)} + C_{n,X}^{(11)} L_X \right) + \frac{\alpha_s^2}{\pi^2} \left(C_{n,X}^{(20)} + C_{n,X}^{(21)} L_X + C_{n,X}^{(22)} L_X^2 \right) \\ &\quad + \frac{\alpha_s^3}{\pi^3} \left(C_{n,X}^{(30)} + C_{n,X}^{(31)} L_X + C_{n,X}^{(32)} L_X^2 + C_{n,X}^{(33)} L_X^3 \right) + \dots \end{aligned} \quad (4)$$

where we have introduced

$$L_X \equiv \log \frac{\mu^2}{m_X^2} \quad (5)$$

In the on-shell scheme we use the notation $C_n^{(kl)} \equiv C_{n,\text{OS}}^{(kl)}$ and we have $C_n^{(11)} = C_n^{(22)} = C_n^{(33)} = 0$. The logarithmic coefficients of order α_s^k , i.e. $C_{n,X}^{(kl)}$ with $l \geq 1$, can be predicted from the lower order coefficients of order α_s^m , $m < k$. The three-loop coefficients $C_{n,X}^{(20)}$ have been computed up to $n = 8$ in Ref. [2] and later up to $n = 30$ in Ref. [3]. The four-loop coefficient $C_{1,X}^{(30)}$ is also known [4, 5] but for $n > 1$ these coefficients have not yet been computed.

The relation between $C_{n,X}^{(kl)}$ and $C_n^{(kl)}$, the coefficients in the scheme X and the on-shell scheme respectively, where the corresponding masses (we denote the pole mass by $m \equiv m_{\text{OS}}$) are related by

$$m = m_X \left(1 + \frac{\alpha_s}{\pi} \delta m_X^{(1)} + \frac{\alpha_s^2}{\pi^2} \delta m_X^{(2)} + \frac{\alpha_s^3}{\pi^3} \delta m_X^{(3)} + \dots \right) \quad (6)$$

is given by

$$C_{n,X}^{(0)} = C_n^{(0)} \quad (7)$$

$$C_{n,X}^{(1)} = C_n^{(10)} - 2n C_n^{(0)} \delta m_X^{(1)} \quad (8)$$

$$\begin{aligned} C_{n,X}^{(2)} &= C_n^{(20)} + C_n^{(21)} L_X - 2n C_n^{(10)} \delta m_X^{(1)} \\ &\quad + \left[n(1+2n)(\delta m_X^{(1)})^2 - 2n \delta m_X^{(2)} \right] C_n^{(0)} \end{aligned} \quad (9)$$

$$\begin{aligned} C_{n,X}^{(3)} &= C_n^{(30)} + C_n^{(31)} L_X + C_n^{(32)} L_X^2 - 2n \delta m_X^{(1)} [C_n^{(20)} + C_n^{(21)} L_X] \\ &\quad - 2 C_n^{(21)} \delta m_X^{(1)} + \left[n(1+2n)(\delta m_X^{(1)})^2 - 2n \delta m_X^{(2)} \right] C_n^{(10)} \\ &\quad - \frac{2n}{3} \left[(1+n)(1+2n)(\delta m_X^{(1)})^3 - 3(1+2n) \delta m_X^{(1)} \delta m_X^{(2)} + 3 \delta m_X^{(3)} \right] C_n^{(0)} \end{aligned} \quad (10)$$

It is clear that these relations break down for large n , due to the terms of order $(n\alpha_s)^k$. In fact, the behaviour for $n \rightarrow \infty$ seems to be even worse than

$n^{-3/2}(\alpha_s\sqrt{n})^l$ as mentioned in the introduction. This is due to the shift in the mass scheme. To be precise, C_n , the coefficients in the on-shell scheme behave like $n^{-3/2}(\alpha_s\sqrt{n})^l$ for $n \rightarrow \infty$. For any threshold scheme X , the factors $\delta m_X^{(l)}$ have to have an additional suppression $\delta m_X^{(l)} \sim \alpha_s$ in order not to destroy the behaviour $n^{-3/2}(\alpha_s\sqrt{n})^l$ for $n \rightarrow \infty$. For the $\overline{\text{MS}}$ -scheme this is not the case and, as we will see, this scheme is particularly inappropriate for large n .

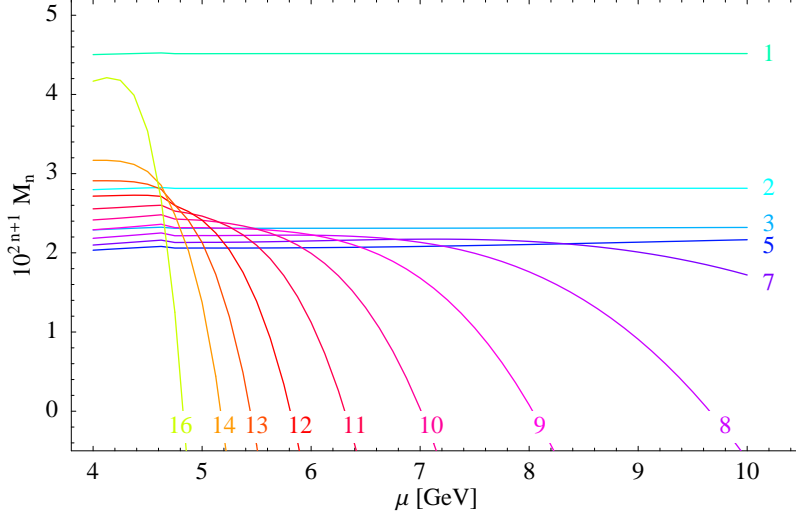


Figure 1: Scale dependence of (some of) the first 16 moments in the $\overline{\text{MS}}$ -scheme. The moments are evaluated with $\overline{m} = 4.184$ GeV in a fixed-order approach including terms up to $\mathcal{O}(\alpha_s^3)$.

In order to substantiate this point consider the scale dependence of the first 16 moments evaluated in a fixed-order approach up to $\mathcal{O}(\alpha_s^3)$ in the $\overline{\text{MS}}$ -scheme. The n -th moment has mass dimensions $[m_b]^{-2n}$ and the moments in this paper are always given in units $[\text{GeV}]^{-2n}$. Since $C_{n,\overline{\text{MS}}}^{(30)}$ is not known for $n > 1$ we set $C_{n,\overline{\text{MS}}}^{(30)} = C_{1,\overline{\text{MS}}}^{(30)}$. We fix $\overline{m} \equiv m_{\overline{\text{MS}}}(m_{\overline{\text{MS}}}) = 4.184$ GeV and then evaluate $m_{\overline{\text{MS}}}(\mu)$ using the renormalization-group equations to four-loop accuracy [18]. We then use this value for the mass and the scale μ to evaluate $M_{n,\overline{\text{MS}}}$ and vary the scale in the region $4 \text{ GeV} \leq \mu \leq 10 \text{ GeV}$. As can be seen in Figure 1, for $n \leq 6$ the moments are very stable for the whole range of μ , but for larger values of n the scale dependence deteriorates rapidly and it is clear that for $n \geq 8$ no information can be extracted from these results any longer. The precise shape of the curves in Figure 1 depends to some extent on details as how to treat the flavour threshold and the value of $C_{n,\overline{\text{MS}}}^{(30)}$, but the main point is not affected by these issues.

The same exercise can be repeated for a threshold mass. As discussed above in this case we would expect a somewhat better behaviour for large n . To investigate this, we use the PS-scheme [14] and set $m_{\text{PS}} \equiv m_{\text{PS}}(\mu_F = 2 \text{ GeV}) = 4.505$ GeV

which, using three-loop conversion, corresponds to $\overline{m} = 4.184$ GeV. Since $\delta m_{\text{PS}}^{(1)} = C_F \mu_F / m_{\text{PS}}$ we have to choose the factorization scale $\mu_F \sim m_b \alpha_s$ to ensure the additional suppression $\delta m_X^{(l)} \sim \alpha_s$ mentioned above and the standard choice is $\mu_F = 2$ GeV. Again we evaluate the first 16 moments varying the scale in the region $2.5 \text{ GeV} \leq \mu \leq 20 \text{ GeV}$. The results depicted in Figure 2 show a remarkable stability with respect to the scale variation. The scale dependence does increase for increasing n but remains in much better control than in the $\overline{\text{MS}}$ -scheme.

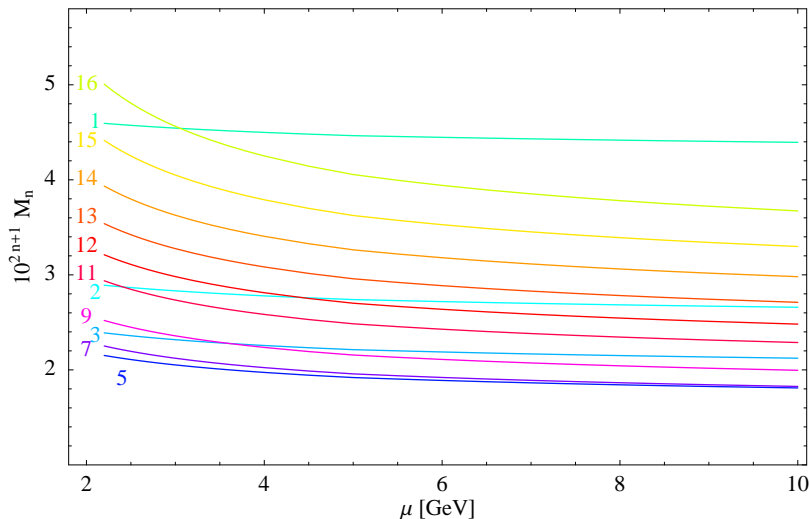


Figure 2: Scale dependence of (some of) the first 16 moments in the PS-scheme with $m_{\text{PS}} = 4.505$ GeV. The moments are evaluated in a fixed-order approach including terms up to $\mathcal{O}(\alpha_s^3)$.

Even though the results shown in Figures 1 and 2 nicely confirm our expectations it is clear that even in the PS-scheme the results become unreliable for large n . To obtain a more complete picture we now turn to the evaluation of the moments in the non-relativistic effective-theory approach and compare these results with the fixed-order results of this section.

3 Effective theory results, large n

As mentioned in the introduction, in the effective-theory approach we start from the Schrödinger equation describing a non-relativistic heavy quark pair with energy $E = \sqrt{s} - 2m_b$ interacting through the potential $-C_F \alpha_s / r$. The cross section $R(s)$ is related to the imaginary part of the corresponding Green function at the origin. Working in dimensional regularization in $d = 4 - 2\epsilon$ dimensions and

minimally subtracting the $1/\epsilon$ ultraviolet singularity, the leading order Coulomb Green function at the origin is given by [19]

$$G_c^{(0)}(0, 0; E) = -\frac{\alpha_s C_F m_b^2}{4\pi} \left(\frac{1}{2\lambda} + \frac{1}{2} \log \frac{-4m_b E}{\mu^2} - \frac{1}{2} + \gamma_E + \psi(1 - \lambda) \right) \quad (11)$$

where $\lambda \equiv C_F \alpha_s / (2\sqrt{-E/m_b})$ and the leading-order cross section is given by

$$R(E) = 6\pi N_c \frac{e_b^2}{m_b^2} \text{Im} [G_c(0, 0; E)] \quad (12)$$

Higher-order corrections are computed by perturbative insertions of higher-order corrections to the potential. The moments are then evaluated performing the integration indicated in Eq. (1). In the literature different options on how to treat the prefactor $1/s^{n+1}$ have been used. Either, this factor can be expanded, writing

$$M_n = \int_{-\infty}^{\infty} \frac{2 dE}{(2m_b)^{2n+1}} e^{-\frac{nE}{m_b}} \left(1 - \frac{E}{2m_b} + \frac{nE^2}{(2m_b)^2} + \dots \right) R(E) \quad (13)$$

where the ellipses stand for higher-order terms in the non-relativistic expansion, or it can be left unexpanded

$$M_n = \int_{-\infty}^{\infty} \frac{2 dE}{(E + 2m_b)^{2n+1}} R(E) \quad (14)$$

Eqs. (13) and (14) agree at NNLO in the effective theory, but will differ considerably for small n . In this section we will use the strictly expanded approach, Eq. (13), but we will come back to this issue in Section 4.

In Figure 3 we show the scale dependence of (some of) the first 16 moments evaluated in the effective theory with $m_{\text{PS}} = 4.505$ GeV. These results are complete at NNLO. Thus, counting $\alpha_s \sim 1/\sqrt{n}$ they include all terms scaling like $n^{-3/2} (\alpha_s \sqrt{n})^l \alpha_s^2$. Furthermore large logarithms are resummed counting $\alpha_s \log n \sim 1$. The results presented here are complete at next-to-leading logarithmic (NLL) accuracy and contain some known contributions at next-to-next-to-leading logarithmic (NNLL) accuracy [12]. The scale dependence of the first few moments is very strong, indicating the expected breakdown of the ET approach for small n . However, for $n \gtrsim 5$ the results are very stable. Increasing n further to $n \gtrsim 14$ leads to an enhanced scale dependence. This is not unexpected, since missing higher-order and NNLL terms as well as non-perturbative corrections become increasingly important.

Of course, the scale dependence is at best a very rough indicator of the reliability of the results. In the following section we will combine the results of Sections 2 and 3, including all terms $\mathcal{O}(\alpha_s^3)$ of the FO approach and all (known) NNLL terms of the ET approach and investigate the relative importance of the various corrections.

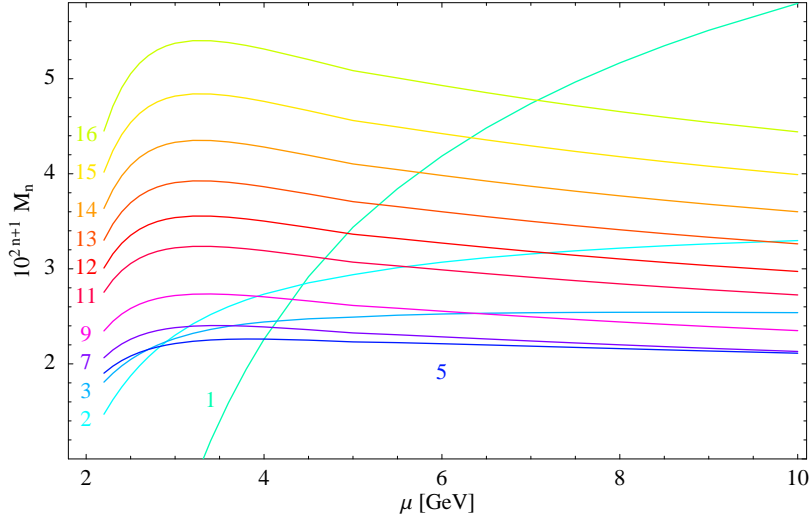


Figure 3: Scale dependence of (some of) the first 16 moments in the PS-scheme with $m_{\text{PS}} = 4.505$ GeV. The moments are evaluated in an effective-theory approach including terms up to NNLL accuracy.

4 Combined analysis

In this section we present the results of a combined approach, i.e. results that are complete at $\mathcal{O}(\alpha_s^3)$ in the FO approach and complete at NNLL in the ET approach. The results are obtained simply by adding the FO and ET results and subtracting the doubly counted terms. In order to obtain the doubly counted terms we expand the ET result in the coupling α_s and retain all terms of $\mathcal{O}(\alpha_s^3)$. Note that these terms depend on the precise implementation of the non-relativistic expansion. In particular, they depend on whether Eq. (13) or Eq. (14) is used. Any implementation that is equivalent at large n of the ET result can be used, as long as the subtraction terms are treated consistently.

Using the implementation according to Eq. (13) and expanding the ET result in α_s leads to integrals of the form

$$\int_{-\infty}^{\infty} \frac{2 dE}{(2m_b)^{2n+1}} e^{-\frac{nE}{m_b}} \text{Im} \left[\left(\frac{m_b}{-E} \right)^x \log^k \left(\frac{-E m_b}{\mu^2} \right) \right] \quad (15)$$

for the corresponding contribution to M_n , where $E = E + i0^+$ is understood. These integrals can either be computed numerically or obtained analytically by differentiation with respect to y of

$$\mathcal{I}_{\text{exp}}(n, x, y) \equiv \int_{-\infty}^{\infty} \frac{2 dE}{(2m_b)^{2n+1}} e^{-\frac{nE}{m_b}} \text{Im} \left[\left(\frac{m_b}{-E} \right)^x \left(\frac{-E m_b}{\mu^2} \right)^y \right] \quad (16)$$

$$= \frac{\pi}{(2m_b)^{2n}} \left(\frac{m_b^2}{\mu^2} \right)^y \frac{n^{-1+x-y}}{\Gamma(x-y)}$$

The corresponding integral using the implementation according to Eq. (14) is given by

$$\begin{aligned} \mathcal{I}_{\text{std}}(n, x, y) &\equiv \int_{-\infty}^{\infty} \frac{2 dE}{(E + 2m_b)^{2n+1}} \text{Im} \left[\left(\frac{m_b}{-E} \right)^x \left(\frac{-E m_b}{\mu^2} \right)^y \right] \\ &= \frac{\pi}{(2m_b)^{2n}} \left(\frac{m_b^2}{\mu^2} \right)^y \frac{2^{1-x+y} \Gamma(x-y+2n)}{\Gamma(2n+1)\Gamma(x-y)} \end{aligned} \quad (17)$$

In the derivation of these results we assumed that μ is independent of E .

n	1	2	3	4	5	6	7
‘exact LO’	9.235	5.021	3.998	3.701	3.713	3.914	4.267
$\mathcal{O}(\alpha_s^0)$	5.458	2.377	1.594	1.275	1.124	1.053	1.030
$\mathcal{O}(\alpha_s^1)$	8.294	4.124	3.028	2.600	2.430	2.394	2.445
$\mathcal{O}(\alpha_s^2)$	9.065	4.795	3.704	3.321	3.224	3.287	3.463
$\mathcal{O}(\alpha_s^3)$	9.211	4.976	3.926	3.595	3.561	3.702	3.975
$\mathcal{O}(\alpha_s^4)$	9.233	5.014	3.983	3.676	3.673	3.853	4.176
$\mathcal{O}(\alpha_s^5)$	9.236	5.020	3.995	3.696	3.704	3.899	4.242

Table 1: Comparison of the exact LO result in the effective theory to the expanded results, Eq. (19). All entries are multiplied by 10^{2n+1} .

In order to illustrate the procedure, let us take the leading-order result in the effective theory, given in Eqs. (11) and (12) and expand it in α_s to say $\mathcal{O}(\alpha_s^5)$

$$\begin{aligned} R(E) &= \frac{3}{4} N_c C_F e_b^2 \left(-\frac{1}{\ell} + \alpha_s \left(1 - \log \frac{-4m_b E}{\mu^2} \right) + 2 \alpha_s^2 \ell \psi^{(1)}(1) \right. \\ &\quad \left. - \alpha_s^3 \ell^2 \psi^{(2)}(1) + \frac{1}{3} \alpha_s^4 \ell^3 \psi^{(3)}(1) - \frac{1}{12} \alpha_s^5 \ell^4 \psi^{(4)}(1) + \dots \right) \end{aligned} \quad (18)$$

where we introduced $\ell \equiv \lambda/\alpha_s = C_F/(2\sqrt{-E/m_b})$ and $\psi^{(k)}$ denotes the k -th derivative of the ψ -function. Integrating this series according to Eq. (13), dropping the higher-order terms in E/m_b , we get

$$\begin{aligned} M_n^{(0)} &= \frac{3 n^{-3/2}}{4(2m_b)^{2n}} N_c e_b^2 \left(\sqrt{\pi} + \bar{\alpha} \pi + \bar{\alpha}^2 \sqrt{\pi} \psi^{(1)}(1) \right. \\ &\quad \left. - \bar{\alpha}^3 \frac{\pi}{4} \psi^{(2)}(1) + \bar{\alpha}^4 \frac{\sqrt{\pi}}{12} \psi^{(3)}(1) - \bar{\alpha}^5 \frac{\pi}{192} \psi^{(4)}(1) + \dots \right) \end{aligned} \quad (19)$$

with $\bar{\alpha} \equiv C_F(\alpha_s\sqrt{n})$. We can now check how the expanded result, Eq. (19) approaches the ‘exact’ leading-order result in the effective theory. This is done in Table 1, where we show the results of performing according to Eq. (13) the integration of $R(E)$ as given in Eq. (12). As in the derivation of Eq. (19) we drop higher-order terms in E/m_b and, for convenience, multiply by 10^{2n+1} . The results for $n \leq 7$ with $m_b = 4.505$ GeV and $\mu = 4.5$ GeV are shown in the second row, labelled ‘exact LO’. The other rows contain the successive approximations given in Eq. (19), with $\alpha_s \equiv \alpha_s(\mu = 4.5 \text{ GeV}) = 0.2198$. As expected, the expanded results approach the ‘exact result’ faster for smaller values on n . Including all terms up to $\mathcal{O}(\alpha_s^3)$ the relative error is $\{0.3\%, 0.9\%, 1.8\%, 3.0\%, 4.3\%, 5.7\%, 7.4\%\}$ for $n = \{1, 2, 3, 4, 5, 6, 7\}$ respectively. The doubly counted terms to be subtracted in the combined analysis at this order correspond to the terms given in the row labelled $\mathcal{O}(\alpha_s^3)$.

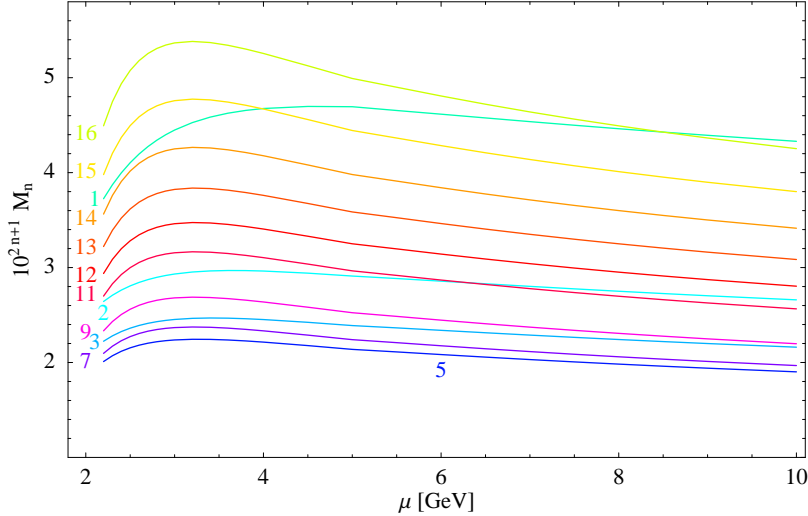


Figure 4: Scale dependence of the first 16 moments in the PS-scheme with $m_{\text{PS}} = 4.505$ GeV. The moments are evaluated in a combined approach including terms up to NNLL accuracy and order $\mathcal{O}(\alpha_s^3)$.

Repeating this exercise with the full NNLL effective-theory result and combining the FO and ET results using the definition Eq. (13) we evaluate again the first 16 moments and depict their scale dependence in Figure 4. Comparing Figures 4 and 3 we note that, as expected, the difference is small for large n and large for small n . The FO corrections to the ET results are $\lesssim 5\%$ for $n = 10$ (except for very small scales), increasing to $\lesssim 10\%$ for $n = 4$. For $n \leq 2$ the corrections completely change the shape of the curve, indicating the importance of relativistic corrections to the non-relativistic sum rules. On the other hand, comparing Figures 4 and 2 the situation is just reversed. For small n the corrections are small (except for very small scales) and they increase with increasing

n	1	2	3	4	6	8	10	13	16
$10^{2n+1}M_n$	4.70	2.94	2.42	2.23	2.21	2.42	2.79	3.68	5.13
comb/ET	1.61	1.03	0.98	0.97	0.97	0.97	0.97	0.97	0.99
comb/FO	1.05	1.07	1.09	1.10	1.14	1.16	1.19	1.22	1.24

Table 2: Comparison of the combined evaluation of selected moments M_n with the ET and FO approach. The moments are evaluated with $m_{\text{PS}} = 4.505$ GeV with the scale $\mu = 4.5$ GeV.

n indicating the importance of resumming terms $(\alpha_s\sqrt{n})^l$ for large n . This is also confirmed by Table 2, where we list the value of some combined moments (second row), as well as the ratio of the combined moment to the ET result (third row) and FO result (fourth row) respectively. We should stress that the ratios in Table 2 depend on the scale choice $\mu = 4.5$ GeV and only give an incomplete picture. In particular, the corrections to the ET result for $n \in \{2, 3, 4\}$ are larger than what might be inferred from Table 2. This is illustrated in Figure 5 where the scale dependence of the second moment is plotted and compared to the experimental moment with its error, indicated by the black line and the grey rectangle. The FO result is plotted as the light blue line. The ET result is evaluated using Eq. (13) (solid dark blue line) and Eq. (14) (dashed dark blue line). As mentioned above, the two implementations differ considerably (for small n). However, the corresponding combined results, depicted as solid and dashed magenta lines respectively, are virtually independent of the implementation, since differences in treating higher-order in n terms are compensated for by adding the full n dependence up to $\mathcal{O}(\alpha_s^3)$ through the FO result. From Figure 5 we can also see that the value of 1.03 given in Table 2 for the ratio of the combined and ET result for the second moment is a coincidence of the scale choice $\mu = 4.5$ GeV and not necessarily indicative of the typical size of the corrections.

The experimental moments used in Figure 5 and the following plots have been determined by taking into account M_n^{res} , the contribution due to the six lowest resonances, and using perturbative QCD in the region $\sqrt{s} > 11.2$ GeV to obtain the continuum contribution M_n^{cont} . This follows closely Ref. [7] from which we also adopt the treatment of M_n^{lin} , the additional contribution in the region $\sqrt{s} > 11.2$ GeV. Due to the uncertainty and the lack of precise experimental data in the region around and just above threshold we add the errors linearly. The experimental moments and their errors are listed in Table 3. The first four moments agree within errors with those given in Ref. [6], but our experimental moments have a larger error.

In order to get a better understanding of the relative importance of the var-

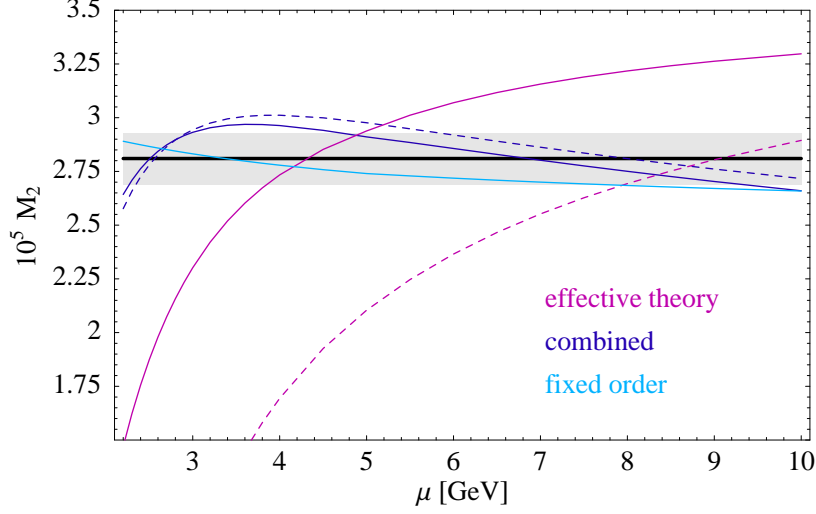


Figure 5: Scale dependence of the second moment in the PS-scheme evaluated using a FO (light blue curve), ET (magenta curves) and a combined approach (dark blue curves). The dashed curves have been obtained using Eq. (13), whereas the solid curves have been obtained using Eq. (14).

n	1	2	3	4	6	8	10	13	16
$10^{2n+1} M_n^{\text{exp}}$	4.51	2.81	2.31	2.13	2.11	2.30	2.64	3.40	4.53
$10^{2n+1} \delta M_n^{\text{exp}}$	0.15	0.12	0.10	0.08	0.07	0.06	0.06	0.06	0.07

Table 3: Values of some selected experimental moments and their errors.

ious corrections and the range of applicability of the various approximations we compare the first 16 moments in the PS-scheme to the experimental moments. We evaluate the moments in the FO, ET and combined approach as well as in the $\overline{\text{MS}}$ fixed-order approach. Note that $\overline{m} = 4.184$ GeV has been determined by requiring the first moment in the $\overline{\text{MS}}$ fixed-order approach to agree with the experimental value. This then fixes $m_{\text{PS}} = 4.505$ GeV and all further moments. For the PS-scheme we vary the scale in the range $2.5 \text{ GeV} \leq \mu \leq 10 \text{ GeV}$, whereas for the $\overline{\text{MS}}$ scheme we vary the scale in the range $4 \text{ GeV} \leq \mu \leq 10 \text{ GeV}$ as explained in Section 1. The results are shown in Figure 6. Note that the scale $\mu = 4.5$ GeV chosen in Table 2 is close to the upper end of the scale variation shown in Figure 6. This explains why the values in Table 2 are generically larger than the experimental moments given in Table 3. The most striking feature of Figure 6 is that in the PS-scheme all three approaches give very similar results.

In particular, the FO approach gives good results even for $n = 16$. The ET approach seems to be valid down to $n = 3$ and only breaks down for $n \lesssim 2$. We note this seems to be a general feature of any suitably defined threshold mass. In particular, we have checked that for the RS-mass [15] the results are very similar. On the other hand, the situation is rather different in the $\overline{\text{MS}}$ scheme. The FO approach gives excellent results for $n \lesssim 7$ and then breaks down abruptly. This can also be inferred from Figure 1. Had we chosen to limit the scale variation by say $\mu < 7$ GeV we would have obtained good results up to $n = 9$.

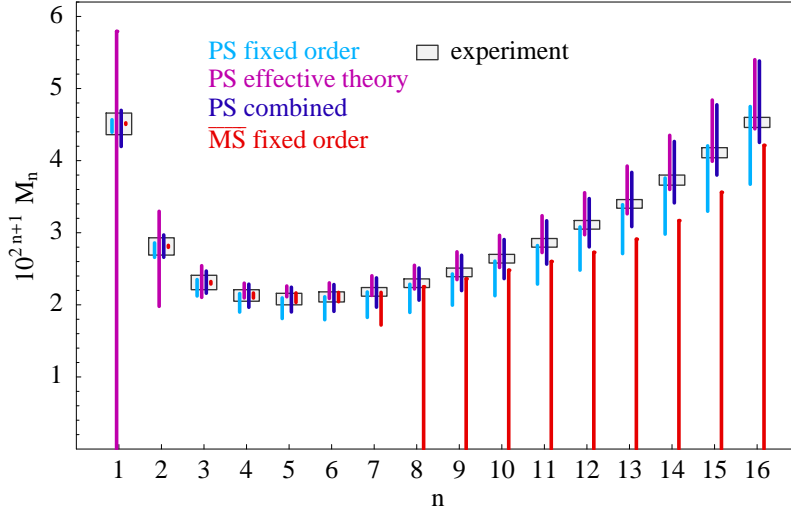


Figure 6: Comparison of the experimental moments to the PS-scheme calculation in a FO approach (left/light blue bands), in an ET approach (middle/magenta bands) and in a combined approach (right/dark blue bands). The bands have been obtained by varying $2.5 \text{ GeV} \leq \mu \leq 10 \text{ GeV}$. Similar bands for the $\overline{\text{MS}}$ -scheme are shown in red.

Finally, we present a similar plot for the OS scheme. We fix the value of the pole mass to make the first moment in the FO approach to agree with the experimental moment. This results in $m = 4.85 \text{ GeV}$. Then we proceed as in the case of the PS scheme. As mentioned at the beginning, the OS scheme is not well suited for a precise determination of quark masses and we would expect the results to be less consistent than with other mass definitions. This is what we find in Figure 7. The FO results are inconsistent with the experimental values of the moments for $n \geq 6$. Accordingly, the corrections $(\alpha_s \sqrt{n})^l$ are more important than in the PS scheme and bring the combined results into agreement with the ET results and the experimental values. The ET results agree with the experimental moments for all values of n , but for $n = 1$ the scale dependence is enormous, making the result meaningless. Overall, the scale dependence is considerably larger than in the PS scheme, in agreement with our expectations.

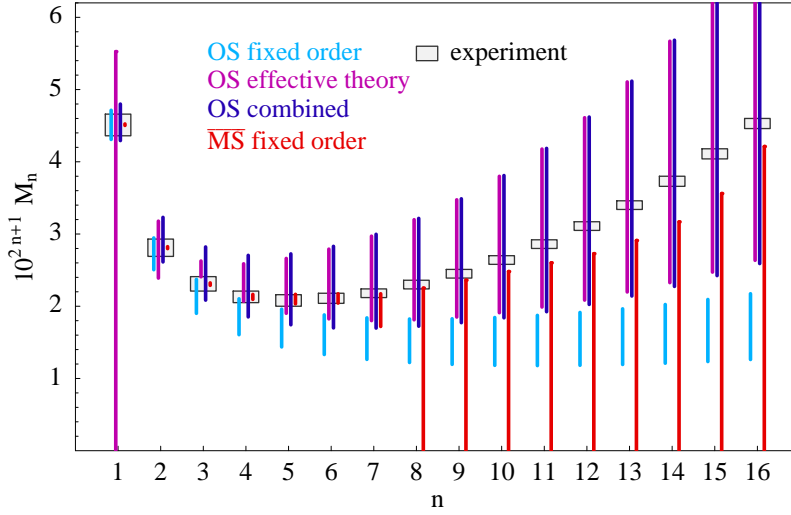


Figure 7: Comparison of the experimental moments to the moments computed in the OS scheme with the pole mass set to $m = 4.85$ GeV in a FO approach (left/light blue bands), in an ET approach (middle/magenta bands) and in a combined approach (right/dark blue bands). The bands have been obtained by varying $2.5 \text{ GeV} \leq \mu \leq 10 \text{ GeV}$. Similar bands for the $\overline{\text{MS}}$ -scheme are shown in red.

5 Conclusions and outlook

The main result of this analysis is that there is no need to make the standard separation into large- n and small- n analyses of the $b\bar{b}$ sum rules. For a suitably defined threshold mass, the fixed-order results are remarkably consistent even for large values of n . With hindsight one might argue that from a numerical point of view the expected breakdown does not happen at $\alpha_s\sqrt{n} \sim 1$ but rather at $(\alpha_s/\pi)\sqrt{n} \sim 1$. Even in the case of the $\overline{\text{MS}}$ -mass where the large- n behaviour is worse due to the presence of terms $(\alpha_s n)^l$, a fixed-order approach is applicable for values of n up to $n \simeq 6$. On the other hand the non-relativistic sum rule can also be applied for values of n that are much smaller than what naively could have been expected. Overall, we obtain a very consistent picture. With the availability of the NNNLO corrections in the effective theory [20] and the prospect of complete results in the fixed-order approach at $\mathcal{O}(\alpha_s^3)$ also for $n > 1$, the sum rule is likely to be the observable of choice for bottom quark mass determinations. Due to the large range of n that can be used, non-perturbative corrections are well under control and additional effects such as non-vanishing charm mass [21, 8] can be included as well. In view of the progress on the theoretical side, more precise experimental data of the b -quark cross section just above threshold would be most welcome.

Acknowledgement

This work is supported in part by the European Community's Marie-Curie Research Training Network under contract MRTN-CT-2006-035505 'Tools and Precision Calculations for Physics Discoveries at Colliders'.

References

- [1] V. A. Novikov *et al.*, Phys. Rev. Lett. **38**, 626 (1977) [Erratum-ibid. **38**, 791 (1977)].
- [2] K. G. Chetyrkin, J. H. Kuhn and M. Steinhauser, Nucl. Phys. B **505**, 40 (1997) [arXiv:hep-ph/9705254].
- [3] R. Boughezal, M. Czakon and T. Schutzmeier, Nucl. Phys. Proc. Suppl. **160**, 160 (2006) [arXiv:hep-ph/0607141].
- [4] K. G. Chetyrkin, J. H. Kuhn and C. Sturm, Eur. Phys. J. C **48**, 107 (2006) [arXiv:hep-ph/0604234].
- [5] R. Boughezal, M. Czakon and T. Schutzmeier, Phys. Rev. D **74**, 074006 (2006) [arXiv:hep-ph/0605023].
- [6] J. H. Kuhn, M. Steinhauser and C. Sturm, arXiv:hep-ph/0702103.
- [7] J. H. Kuhn and M. Steinhauser, Nucl. Phys. B **619**, 588 (2001) [Erratum-ibid. B **640**, 415 (2002)] [arXiv:hep-ph/0109084].
- [8] G. Corcella and A. H. Hoang, Phys. Lett. B **554**, 133 (2003) [arXiv:hep-ph/0212297].
- [9] N. Brambilla, A. Pineda, J. Soto and A. Vairo, Rev. Mod. Phys. **77**, 1423 (2005).
- [10] K. Melnikov and A. Yelkhovsky, Phys. Rev. D **59**, 114009 (1999) [arXiv:hep-ph/9805270];
A. A. Penin and A. A. Pivovarov, Nucl. Phys. B **549**, 217 (1999) [arXiv:hep-ph/9807421];
A. H. Hoang, Phys. Rev. D **61**, 034005 (2000) [arXiv:hep-ph/9905550];
M. Beneke and A. Signer, Phys. Lett. B **471** (1999) 233 [arXiv:hep-ph/9906475].
- [11] A. H. Hoang, A. V. Manohar, I. W. Stewart and T. Teubner, Phys. Rev. Lett. **86**, 1951 (2001) [arXiv:hep-ph/0011254];
A. Pineda, Phys. Rev. D **66**, 054022 (2002) [arXiv:hep-ph/0110216];

- A. Pineda, Phys. Rev. D **65**, 074007 (2002) [arXiv:hep-ph/0109117];
A. H. Hoang, Phys. Rev. D **69**, 034009 (2004) [arXiv:hep-ph/0307376];
A. Pineda and A. Signer, Nucl. Phys. B **762**, 67 (2007) [arXiv:hep-ph/0607239].
- [12] A. Pineda and A. Signer, Phys. Rev. D **73**, 111501 (2006) [arXiv:hep-ph/0601185].
- [13] I. I. Y. Bigi, M. A. Shifman and N. Uraltsev, Ann. Rev. Nucl. Part. Sci. **47**, 591 (1997) [arXiv:hep-ph/9703290];
A. H. Hoang, Z. Ligeti and A. V. Manohar, Phys. Rev. Lett. **82**, 277 (1999) [arXiv:hep-ph/9809423].
- [14] M. Beneke, Phys. Lett. B **434**, 115 (1998) [arXiv:hep-ph/9804241].
- [15] A. Pineda, JHEP **0106**, 022 (2001) [arXiv:hep-ph/0105008].
- [16] M. A. Shifman, A. I. Vainshtein and V. I. Zakharov, Nucl. Phys. B **147**, 385 (1979).
- [17] D. J. Broadhurst, P. A. Baikov, V. A. Ilyin, J. Fleischer, O. V. Tarasov and V. A. Smirnov, Phys. Lett. B **329**, 103 (1994) [arXiv:hep-ph/9403274].
- [18] K. G. Chetyrkin, J. H. Kuhn and M. Steinhauser, Comput. Phys. Commun. **133**, 43 (2000) [arXiv:hep-ph/0004189].
- [19] M. Beneke, A. Signer and V. A. Smirnov, Phys. Lett. B **454**, 137 (1999) [arXiv:hep-ph/9903260];
M. Beneke, in: Proceedings of the 8th International Symposium on Heavy Flavor Physics (Heavy Flavors 8), Southampton, England, 25-29 Jul 1999, [arXiv:hep-ph/9911490].
- [20] M. Beneke, Y. Kiyo and K. Schuller, Nucl. Phys. B **714**, 67 (2005) [arXiv:hep-ph/0501289];
M. Beneke, Y. Kiyo and K. Schuller, arXiv:0705.4518 [hep-ph];
M. Beneke, Y. Kiyo and A. A. Penin, arXiv:0706.2733 [hep-ph].
- [21] A. H. Hoang, J. H. Kuhn and T. Teubner, Nucl. Phys. B **452**, 173 (1995) [arXiv:hep-ph/9505262];
K. G. Chetyrkin, A. H. Hoang, J. H. Kuhn, M. Steinhauser and T. Teubner, Eur. Phys. J. C **2**, 137 (1998) [arXiv:hep-ph/9711327].